

See discussions, stats, and author profiles for this publication at: <https://www.researchgate.net/publication/230795551>

Infrared Spectroscopy of the Mass 31 Cation: Protonated Formaldehyde vs Methoxy

ARTICLE in THE JOURNAL OF PHYSICAL CHEMISTRY A · SEPTEMBER 2012

Impact Factor: 2.69 · DOI: 10.1021/jp3072298 · Source: PubMed

CITATIONS

6

READS

50

4 AUTHORS, INCLUDING:



Jonathan D Mosley

United States Environmental Protection Agency

12 PUBLICATIONS 40 CITATIONS

SEE PROFILE

Infrared Spectroscopy of the Mass 31 Cation: Protonated Formaldehyde vs Methoxy

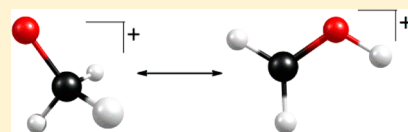
J. D. Mosley,[†] T. C. Cheng,[†] A. B. McCoy,[‡] and M. A. Duncan^{*,†}

[†]Department of Chemistry, University of Georgia, Athens, Georgia 30602, United States

[‡]Department of Chemistry, The Ohio State University, Columbus, Ohio 43210, United States

S Supporting Information

ABSTRACT: Pulsed discharges containing methanol or ethanol produce ions having the nominal formula $[\text{C}_2\text{H}_3\text{O}]^+$, i.e. $m/z = 31$. Similar ions resulting from electron impact ionization in mass spectrometers are long recognized to have either the CH_2OH^+ protonated formaldehyde or CH_3O^+ methoxy cation structures. The H_2OCH^+ oxonio-methylene structure has also been suggested by computational chemistry. To investigate these structures, ions are expanded in a supersonic beam, mass-selected in a time-of-flight spectrometer, and studied with infrared laser photodissociation spectroscopy. Sharp bands in the O–H and C–H stretching and fingerprint regions are compared to computational predictions for the three isomeric structures and their vibrational spectra. Protonated formaldehyde is the most abundant isomer, but methoxy is also formed with significant abundance. The branching ratio of these two ion species varies with precursors and formation conditions.



INTRODUCTION

Throughout the history of mass spectrometry, determination of the structures of cations resulting from molecular ionization and fragmentation has been a central focus.^{1,2} The reactivity of ions and their dissociation energetics and dynamics provide indirect probes of structure.^{1,2} However, ion spectroscopy, which can provide direct structural information, is difficult because of the extreme conditions and mixtures present in plasmas and the low densities of ions produced.^{3–5} Computational studies exploring ion structures reveal the occurrence in many systems of more than one isomeric structure lying at accessible energies.^{1–5} Small cation structures and their reactions are also of significant interest for interstellar chemistry.^{6–9} Recent developments in ion spectroscopy have made it possible to obtain infrared spectra of mass-selected ions via resonance-enhanced photodissociation.^{3–5,10–15} Our group has recently investigated the isomeric structures of several small carbocations with this methodology.^{16–20} C_2H_3^+ was shown to have the nonclassical protonated acetylene structure rather than the classical vinyl cation structure.¹⁶ C_3H_3^+ was found to coexist in both the cyclopropenyl and the propargyl cation isomer structures,¹⁷ and C_3H_5^+ was found to exist as both the allyl and 2-propenyl cations.¹⁸ In the present report, we extend these studies to the isomers of simple oxygen-containing ions having the nominal formula $[\text{C}_2\text{H}_3\text{O}]^+$.

The ion at $m/z = 31$ is produced as an abundant fragment in the ionization of methanol, ethanol, dimethyl ether, and other small oxygen-containing molecules.²¹ This ion has been the subject of much study and discussion in the mass spectrometry community for many years.^{22–42} Two important structures are recognized, the CH_2OH^+ protonated formaldehyde ion and the CH_3O^+ methoxy cation. The HCOH_2^+ oxonio-methylene ion was also proposed on the basis of computational studies,²⁸ but there is apparently no experimental evidence for this species. In

early studies on ions at low temperature, evidence was found for a weakly bound HCO^+-H_2 complex.^{24–26} As shown in Figure 1, protonated formaldehyde has a singlet ground state and is by far the most stable structure. The methoxy cation lies

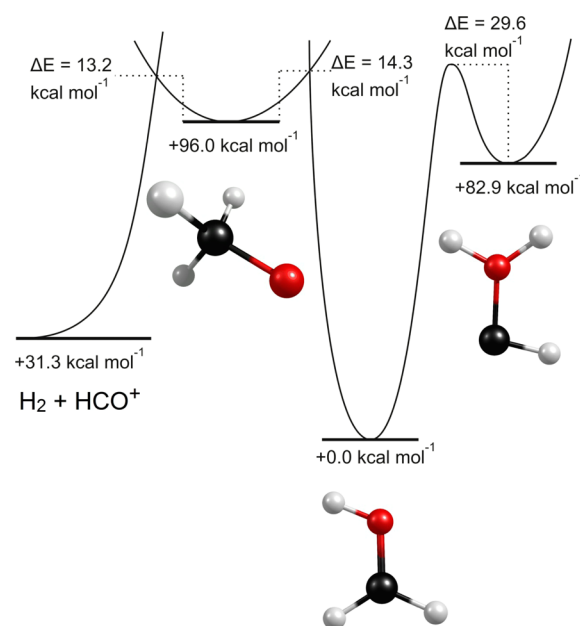


Figure 1. Schematic energy level diagram showing the relative energies of methoxy, protonated formaldehyde, and oxonio-methylene as well as the energies of the curve crossings connecting these species.

Received: July 20, 2012

Revised: September 4, 2012

Published: September 4, 2012

+96.0 kcal/mol above this, with a triplet ground state. Therefore, interconversion of these two ions requires a curve crossing, which has been estimated to lie +14.3 kcal/mol above the methoxy ground state.⁴⁰ Oxonio-methylene is also a singlet, lying +82.9 kcal/mol above protonated formaldehyde.²⁸ The collisional dissociation of a variety of ions having $m/z = 31$ produces fragmentation with an $m/z = 15:14$ peak ratio of about 0.03, suggesting that the most common structure produced is protonated formaldehyde. Different fragmentation (an intense $m/z = 15$ peak) attributed to methoxy cation can be produced by charge reversal of the corresponding anions.^{27,32} Attempts to detect methoxy by ionization of neutral CH_3O radicals from various sources were unsuccessful.³⁷ Instead, HCO^+ ions were detected at a higher photoionization threshold, presumably by prompt fragmentation of the nascent CH_3O^+ . Collisional dissociation of $[\text{C}_2\text{H}_3\text{O}]^+$ proceeds by elimination of H_2 with significant translational energy release.^{35,39–41} However, the energy release is the same for ions believed to have either the CH_3O^+ or CH_2OH^+ structures. This has been interpreted to indicate that methoxy crosses over into the protonated formaldehyde structure before dissociating, although it has also been proposed that methoxy dissociates directly to $\text{HCO}^+ + \text{H}_2$.⁴⁰ The protonated formaldehyde ion has been characterized with gas phase infrared spectroscopy via an O–H stretching band⁴³ and with millimeter wave measurements;⁴⁴ it has also been detected in interstellar space.⁴⁵ The vibrational spectrum of protonated formaldehyde has also been investigated computationally,^{46–49} but there is no spectroscopy of the methoxy cation to our knowledge. Here we describe the infrared spectroscopy of the mass-selected $m/z = 31$ ion, produced via discharge in a supersonic expansion, which shows that *both* protonated formaldehyde and the methoxy cation structures are present.

EXPERIMENTAL DETAILS

Ions for these experiments are produced in a pulsed discharge/supersonic expansion source using needle electrodes, as described previously.^{16–20} The expansion gas is argon seeded with the ambient vapor pressure of methanol or ethanol at room temperature. The discharge is activated for a 5–10 μs duration in the center of a 250–300 μs gas pulse. After this, ions expand supersonically to form a dense, cold plasma. This beam is collimated by a skimmer before sampling by a reflectron time-of-flight mass spectrometer (RTOF) in a differentially pumped chamber.⁵⁰ Ions are extracted perpendicular to their flight direction from the molecular beam into the RTOF. To select specific ions for photodissociation, pulsed deflection plates are employed at the end of the first flight tube section. Ions are excited with the tunable infrared laser in the turning region of the reflectron, and mass analysis of any fragmentation peaks occurs in a second flight tube section.⁵⁰ The IR laser is a Nd:YAG-pumped optical parametric oscillator/amplifier (OPO/OPA; LaserVision). In its normal operating configuration,⁵¹ a KTP oscillator pumped at 532 nm and a KTA difference frequency generation (idler +1064 nm) amplifier provides tunable output in the 2000–4500 cm^{-1} region with a line width of about 1 cm^{-1} . In a second configuration, another stage of difference frequency generation in AgGaSe_2 provides output in the 800–2200 cm^{-1} range.⁵²

Computational studies are carried out at the MP2/cc-pVTZ and DFT/B3LYP levels of theory using the Gaussian03 program package.⁵³ Energetics are reported from the MP2 calculations, whereas vibrational spectra are those from DFT/

B3LYP, taking advantages of the best performance of each method as noted in previous work from our lab.^{16–20} A vibrational scaling factor of 0.9682 was employed for the DFT/B3LYP spectra, as recommended by Radom and co-workers for this level of theory (a factor of 0.9561 was used for MP2 spectra, presented only in the Supporting Information).⁵⁴

RESULTS AND DISCUSSION

Electrical discharges in methanol or ethanol produce a rich mass spectrum containing many fragment ions and their clusters with precursor molecules and with argon. A representative mass spectrum is shown in the Supporting Information. Figure 2 shows the infrared photodissociation

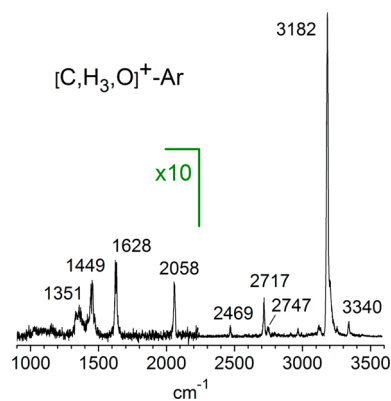


Figure 2. Infrared photodissociation spectrum of the mass 31 cation obtained by tagging it with argon and measuring the argon elimination mass channel.

spectrum measured for the $[\text{C}_2\text{H}_3\text{O}]^+ - \text{Ar}$ ion produced in a discharge of ethanol, when it is mass selected and the photofragment is detected in the mass channel corresponding to argon elimination. An intense resonance near 3182 cm^{-1} dominates the spectrum, but there are vibrational bands throughout the 1000–3500 cm^{-1} region. The 3182 cm^{-1} band is in the region where an O–H stretch is expected for protonated formaldehyde, although this band is shifted significantly to lower energy compared to the O–H stretch seen by Amano and co-workers at 3422.8 cm^{-1} .⁴³ Bands near 2700 cm^{-1} can be associated with C–H stretches, whereas those in the 1000–1600 cm^{-1} region should be CH bending and carbonyl stretching vibrations. To investigate detailed assignments for these bands, we use computational chemistry of the three isomer possibilities for these ions. Table 1 shows the relative energies for the three isomers at both the MP2 and DFT/B3LYP levels of theory. As expected from previous work, protonated formaldehyde is far more stable than either the methoxy or oxonio-methylene ions; the relative energies of the three isomers are completely consistent with previous results.^{22–25,28,30,33,36,40} We have not investigated the energies of the singlet/triplet curve crossing for methoxy/protonated formaldehyde but use here the previous results of Schwarz and co-workers.⁴⁰ The oxonio-methylene energetics shown are those from Radom and co-workers.²⁸

Figure 3 shows an expanded view of the mass 31 ion spectrum compared to the predictions of theory for the protonated formaldehyde, methoxy and oxonio-methylene cations, each with attached argon. The intensities of bands in the computed spectra are those for linear absorption, whereas those in the experiment are determined by the absorption

Table 1. Relative Energies of $[\text{C}_2\text{H}_3\text{O}]^+$ Isomers (kcal/mol) with and without Argon at the DFT/B3LYP and MP2 Levels of Theory with the Correlation Consistent Dunning Triple ζ Basis Set^a

isomer	ΔE (MP2)	ΔE (B3LYP)
CH_2OH^+	0.0	0.0
CHOH_2^+	+81.1	+78.3
CH_3O^+	+91.3	+72.8
$\text{CH}_2\text{OH}^+-\text{Ar}$	0.0	0.0
$\text{CHOH}_2^+-\text{Ar}$	+79.8	+76.9
$\text{CH}_3\text{O}^+-\text{Ar}$ (1)	+93.3	+73.8
$\text{CH}_3\text{O}^+-\text{Ar}$ (2)	+93.7	+75.5
$\text{CH}_3\text{O}^+-\text{Ar}$ (3)	+93.9	+75.1

^aAll energetics are corrected for zero point energy.

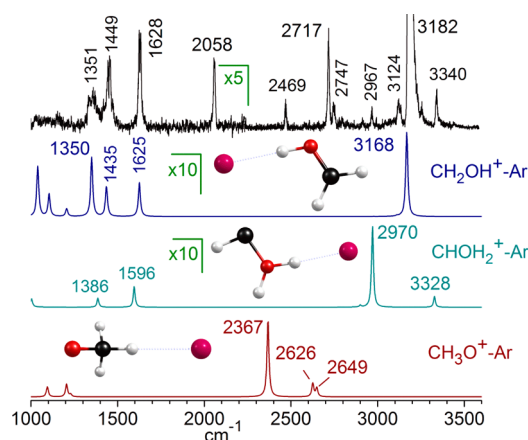


Figure 3. Expanded view of the IR spectrum measured for the mass 31 cation compared to the predictions of theory for protonated formaldehyde (second trace/dark blue), oxonio-methylene cation (third trace/turquoise), and the methoxy cation (bottom trace/dark red). All computations include the argon atom and frequencies are scaled by a factor of 0.9682.⁵⁴

strength, the photodissociation yield, and the IR laser power, which falls gradually toward lower energy. We normalize the data to parent ion intensity variations, but not to the laser power because the beam shape and hence the overlap with the ion beam changes across the spectrum. Therefore, band positions are more significant than intensities, particularly when comparisons are made at different ends of the spectrum.

It is immediately clear that many of the bands here can be assigned to the protonated formaldehyde cation. The strong 3182 cm^{-1} feature is reproduced reasonably well in position and intensity for the O–H stretch vibration. The different position of this band compared to that of the vibration in the isolated ion⁴³ results because the argon atom attaches on the proton, inducing a strong red shift. This can be seen via calculations with and without argon (see Supporting Information), and large red shifts have been seen for other ions with argon attached at a proton site.¹⁶ Just below the 3182 cm^{-1} feature, we see weak bands assigned to the symmetric (2967 cm^{-1}) and asymmetric (3124 cm^{-1}) CH_2 stretches that were not reported previously but agree well with the predictions of theory. The bands at lower frequency for protonated formaldehyde have also not been reported previously, but all have been predicted before with computational chemistry.^{46–49} These include the carbonyl stretch (1628 cm^{-1}), the CH_2 scissors vibration (1449 cm^{-1}), and the COH^+

in-plane hydrogen bend (1351 cm^{-1}). These vibrations are all reproduced well by our theory, which includes the argon, and are in good agreement with previous theory (done without argon),^{46–49} because the shift from the argon is small (see Supporting Information). The photodissociation signal drops off below the 1351 cm^{-1} band, most likely due to the bond energy of the argon tag. This is computed to be 4.4 kcal/mol (1540 cm^{-1}) for protonated formaldehyde at the MP2 level and $1.7\text{--}2.1\text{ kcal/mol}$ for the different argon isomers of methoxy (see Supporting Information and discussion below).

The vibrational frequencies for protonated formaldehyde can be compared to those of formaldehyde itself.⁵⁵ The carbonyl stretch of protonated formaldehyde (1628 cm^{-1}) is shifted to much lower frequency than that in formaldehyde (1746.1 cm^{-1}). This suggests that protonation weakens the $\text{C}=\text{O}$ bond, presumably by withdrawing electron density from it. Consistent with this, the computed $\text{C}=\text{O}$ bond distance in protonated formaldehyde (1.248 Å at the MP2 level) is longer than that in formaldehyde (1.205 Å). Likewise, the CH_2 scissors frequency here (1449 cm^{-1}) is lower than in formaldehyde (1500.1 cm^{-1}), again consistent with a less rigid system. A similar trend is found for the formaldehyde cation,⁵⁵ which also has lower $\text{C}=\text{O}$ (1675 cm^{-1}) and CH_2 scissors (1210 cm^{-1}) vibrations than the neutral. The lower frequency bands at 1351 , 1449 , and 1628 cm^{-1} can also be compared to the vibrations in high Rydberg states of the CH_2OH hydroxymethyl radical that converge to the protonated formaldehyde ground state.^{56–59} As shown in Table 2, each of these vibrations is within a few cm^{-1} of the frequencies seen here.

Table 2. Vibrational Bands of the Mass 31 Cation Tagged with Ar Compared with Theory and Previous Experiments^a

exp	theory (int)	previous exp	assignment
1351	1350 (92.5)	1351^b , 1357^c , 1370^d	in phase HCOH bend (CH_2OH^+)
1449	1435 (47.1)	1459^b , 1465^c	CH_2 scissors (CH_2OH^+)
1628	1625 (53.4)	1623^b , 1621^c , 1650 ± 30^d	$\text{C}=\text{O}$ stretch (CH_2OH^+)
2058	2090 ^e		O–H τ (oop) overtone (CH_2OH^+)
2469	2367 (1028.0)		$\text{C}=\text{H}$ stretch (CH_3O^+)
2717	2626 (181.6)		sym. $\text{C}=\text{H}_2$ stretch (CH_3O^+)
2747	2649 (120.2)		asym. $\text{C}=\text{H}_2$ stretch (CH_3O^+)
2967	2977 (0.9)		sym. CH_2 stretch (CH_2OH^+)
3124	3111 (8.9)		asym. CH_2 stretch (CH_2OH^+)
3182	3168 (1317.7)	3423^f	O–H stretch (CH_2OH^+)
3254			
3340	3356 (36.1)		combination band $\nu_1 + \nu_{11}$ (CH_2OH^+)

^aBand positions are in cm^{-1} ; IR intensities are in km/mol . ^bReference 56. ^cReference 57. ^dReference 58. ^eFrom anharmonic analysis. ^fReference 41.

Bands in the middle of the spectrum are not readily identified as fundamentals of protonated formaldehyde. These include the feature at 2058 cm^{-1} and the group of bands at 2469 , 2717 , and 2747 cm^{-1} . Additionally, a less intense but noticeable band at 3340 cm^{-1} is also not readily assigned. We consider the 2469 , 2717 , and 2747 cm^{-1} group of bands first. Protonated formaldehyde has no vibrations in this region, but the methoxy cation does have bands predicted here, as shown in the lower trace of Figure 3. However, although three bands are predicted

for $\text{CH}_3\text{O}^+\text{Ar}$, the pattern of peak positions and intensities from theory does not match the experiment. Because we use the method of argon tagging, and because argon often binds in more than one position on other ions,⁵⁹ we conducted a careful study of its binding sites on methoxy and their influence on the vibrational patterns (a similar study on protonated formaldehyde found only the Ar-on- H^+ isomer). Three binding sites for argon attached to methoxy correspond to stable minima. Table 1 presents the energetics for these complexes, and Figure 4 shows the spectra for each of these structures compared to

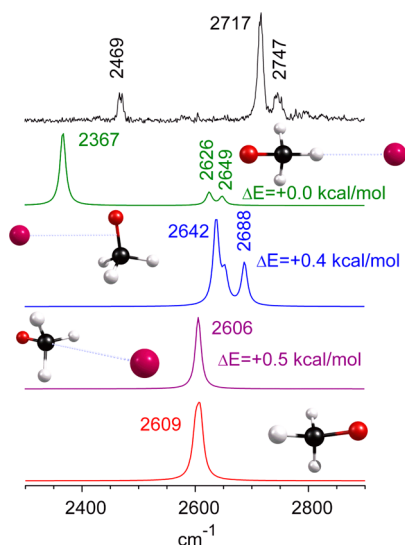


Figure 4. Bands attributed to methoxy cation compared to the spectra predicted for isomers with argon at different binding sites.

the experiment. These include the 3-fold pocket between the CH groups (purple trace in Figure 4), a single CH site (green trace), and along the side of the CO bond (blue trace); the energies of these sites are extremely close. If argon binds in the 3-fold pocket on the C_3 axis, the symmetry of the argon-free system is preserved, and two overlapping C–H stretches are predicted (symmetric and degenerate asymmetric stretch) just as seen for the isolated methoxy cation. If argon binds on a single CH position, the symmetry is broken, and this C–H stretch is red-shifted with respect to the other two, which break into a symmetric/asymmetric CH_2 pair. If argon binds alongside the CO bond, it interacts more strongly with one CH than the others, and a similar splitting produces a unique vibration and a symmetric/asymmetric pair. Unfortunately, none of the vibrational patterns computed for these limiting structures exactly matches the spectrum. The best match is for the Ar-on-CH structure, which is computed to be most stable. It has three bands with about the right spacing, with one more red-shifted than the other two, but the position and relative intensities do not match the spectrum exactly. However, because the energy differences between these sites are so small, it is likely that the potential for argon motion is quite flat and that the argon samples more than one of these configurations. If we recognize that the level of theory employed (and perhaps the scaling factors) is not ideal for such weak interactions, and that the zero point motion may exceed the barriers between argon configurations, it is not too surprising that we do not have an exact match to the experimental spectrum. The Ar-on-CH configuration produces a shifted band and a doublet, which is what we see in the experiment, although the exact spacings

and relative intensities are not perfect. It is likely that this main configuration, and perhaps some dynamical averaging over nearby configurations, can explain the spectrum. We therefore assign the 2469, 2717, and 2747 cm^{-1} bands to the C–H stretches of the methoxy cation.

Detection of a stable methoxy cation living many hundreds of microseconds is surprising in light of the difficulties in producing this species in the past and its high instability relative to protonated formaldehyde. In additional tests to confirm this assignment, we first varied the precursor used to produce the mass 31 cation. Experiments comparing methanol and ethanol produce the spectra shown in Figure 5. As indicated with the

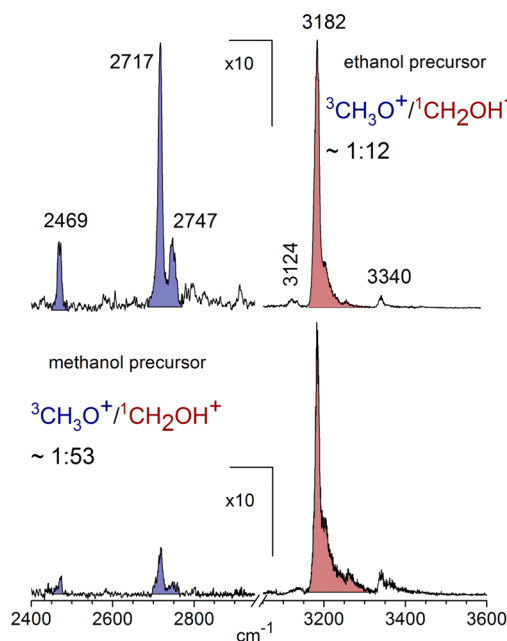


Figure 5. Variation in the bands attributed to methoxy (blue) versus protonated formaldehyde (red) when ions are produced from ethanol versus methanol precursors.

shaded bands, the intensities of the 2469, 2717, and 2747 cm^{-1} bands track together as a group, but the intensity of this group varies significantly with respect to that of the 3182 cm^{-1} band. If these bands were all from the same ion, their relative intensities would remain constant. These data therefore strongly support the assignment of the 2469, 2717, and 2747 cm^{-1} bands to an isomer other than protonated formaldehyde, consistent with our assignment of these bands to methoxy. Using the computed IR intensities of the bands for methoxy versus protonated formaldehyde, and comparing the integrated area of these bands, we can estimate a branching ratio for these two isomers. As shown in the figure, the methoxy:protonated formaldehyde ratio under these discharge conditions is 1:53 for the methanol precursor and 1:12 for the ethanol precursor.

In a second test, we varied the discharge conditions used to produce the ions. We presume that both protonated formaldehyde and methoxy are produced in some initial branching ratios following the energetic ionization/fragmentation process, and that the survival of each depends on its cooling rate and efficiency in our source. In particular, survival of methoxy requires that it be cooled and stabilized behind the barrier at the triplet/singlet curve crossing to protonated formaldehyde. The temperature of the plasma should therefore affect the methoxy/protonated formaldehyde branching ratio. To esti-

mate the temperature, we use the computed rotational constants of protonated formaldehyde tagged with argon to simulate a rotational contour for the O–H stretching band and adjust its line width (fwhm) to match that in the experiment (see simulations in Supporting Information). This procedure is not perfect, as the line width may also have contributions from predissociation, but it is good enough for a rough estimate. Our normal cold discharge/expansion conditions using ethanol lead to a rotational temperature of about 25 K, consistent with ion temperatures measured previously with this source. To change the ion temperature, we increase the discharge voltage level and move its pulse timing relative to the center of the gas pulse. This simultaneously increases the heating of the plasma and spoils the collisional cooling. The comparison of the spectrum obtained with these hotter conditions to that with the normal cold settings is shown in Figure 6. As shown, hotter conditions

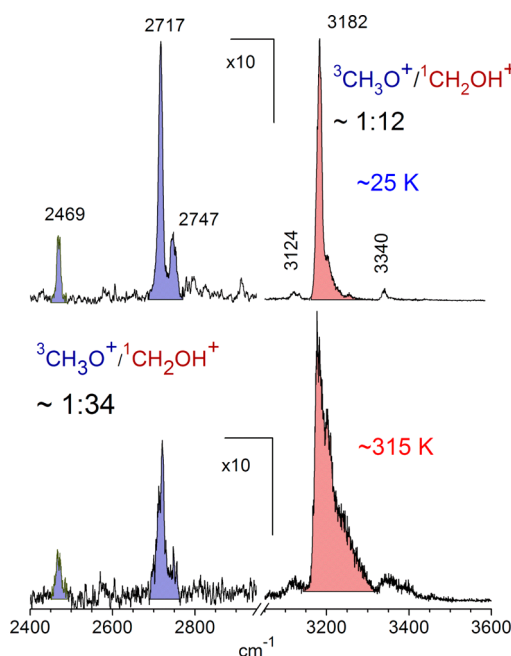


Figure 6. Variation in the bands attributed to methoxy (blue) versus protonated formaldehyde (red) when ions are produced under cold versus hot discharge conditions. Temperatures are estimated from the rotational contour of the O–H stretch of protonated formaldehyde (see Supporting Information).

produce a broader protonated formaldehyde O–H stretching band more shaded to the blue, with a temperature of roughly 315 K. Vibrations are not likely to be equilibrated to this same temperature, but this confirms that the plasma is heated to a significant degree. Corresponding to these conditions, the bands attributed to methoxy decrease in intensity. Again, comparing the integrated areas and computed IR intensities, we arrive at a $\text{CH}_3\text{O}^+:\text{CH}_2\text{OH}^+$ ratio of 1:34. Less methoxy survives at higher temperature, consistent with inefficient trapping behind the singlet/triplet curve crossing barrier. Overall, the dependence on precursor and discharge conditions are consistent with the assignment of the 2469, 2717, and 2747 cm^{-1} bands to an isomer other than protonated formaldehyde. The vibrational analysis indicates that this isomer is methoxy. Its production efficiency is different for different precursors and conditions, consistent with expectations for a metastable species. Because we have been able to capture this ion, the

qualitative aspects of the potential energy surface and singlet/triplet curve crossings proposed previously⁴⁰ must be valid; i.e., there must be a significant local well on the methoxy surface.

The oxonio-methylene cation has been suggested as a possible structural isomer by theory,²⁸ but there is no experimental evidence for this ion to our knowledge. We find a stable minimum for this structure, whose predicted spectrum is shown in the third trace from the top in Figure 3. Vibrations are predicted at 2970 and 3328 cm^{-1} , near experimental bands, but the relative intensities do not match the experiment. Because the IR laser power is steady in this region, measured intensities should resemble those computed. As noted above, the 2967 cm^{-1} band can also be assigned to the weak symmetric CH_2 stretch of protonated formaldehyde. This band is not evident in the theory trace for this ion because it is so much weaker than the O–H stretch. As discussed below, the 3340 cm^{-1} can be assigned to a combination band. Considering all this, it is not possible to completely exclude the presence of a small amount of oxonio-methylene cation, but we conclude that there is no compelling evidence for it.

Unassigned vibrational bands remain at 2058 and 3340 cm^{-1} that are not close to predicted fundamentals of protonated formaldehyde nor methoxy cation. Therefore, we investigate assignments for these features involving overtones or combination bands, guided by past experience with similar systems. Such overtone and combination bands can be quite prominent in ion spectra because of the effects of charge on vibrational couplings and IR intensities. The 2058 cm^{-1} band is at an energy roughly twice that of the harmonic frequency of the $(\text{H}_2)\text{COH}$ out-of-plane torsion for protonated formaldehyde, which is calculated to be 1101 cm^{-1} . If anharmonicity is included in the calculation of the energy of this overtone using second-order vibrational perturbation theory, as implemented in Gaussian03⁵³ at the MP2/6-311+G(d,p) level of theory/basis, the overtone is reduced to 2090 cm^{-1} , close to the position of the unassigned band. To evaluate the feasibility of the assignment of this band to the overtone in the torsion, we performed a one-dimensional scan of the $(\text{H}_2)\text{COH}$ torsion, while requiring that the argon atom remain coplanar with the CH_2 group. As expected, this motion induces a change in the component of the dipole moment along the axis perpendicular to the molecular plane (the c -axis) varying linearly with displacement of the O–H hydrogen atom off of the molecular plane. The dipole moment along the a -axis, which lies nearly parallel to the OH bond in the equilibrium geometry, varies quadratically with the displacement of the $(\text{H}_2)\text{COH}$ torsion. The calculated potential and dipole functions are fit to quadratic polynomials in the displacement of the torsion angle from its value at the minimum energy geometry. These curves are used to evaluate the vibrational wave functions (1-d) and with these the intensities of the fundamental and first overtone in the torsion. This analysis yields an intensity for the overtone transition that is roughly 25% of the fundamental excitation, or comparable in intensity to the three low-frequency fundamentals in the spectrum (Figures 2 and 3). We therefore assign the 2058 cm^{-1} band to the overtone of this out-of-plane torsional band.

The origin of the overtone intensity in the $(\text{H}_2)\text{COH}$ torsion comes from the response of the charge distribution in protonated formaldehyde when the interaction between the charged OH group and the argon is broken. Similar behavior has been reported previously in halide–water clusters.^{60,61} In both systems the fundamental transition arises from the

displacement of a hydrogen atom that carries a large part of the excess charge off of the molecular plane. The overtone comes from the fact that as the interaction between the argon atom and protonated formaldehyde is weakened by displacement of the hydrogen atom off of the molecular plane, the partial charge on argon becomes closer to zero, and the excess charge becomes localized on protonated formaldehyde. The charge redistribution is primarily in the molecular plane and these changes will be the same if the hydrogen is displaced above or below this plane. The angular dependence of the a -component of the dipole moment for bare protonated formaldehyde (red circles) and the complex of protonated formaldehyde with an argon atom (blue circles) are plotted in Figure 7. The

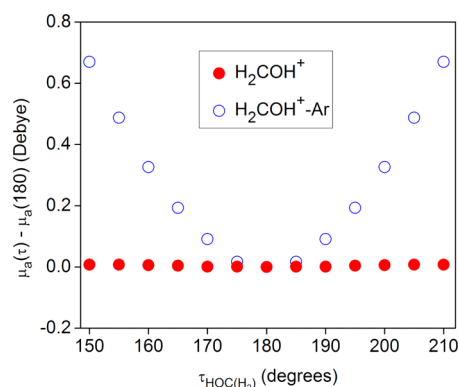


Figure 7. Variation in the component of the dipole moment along the a -axis, plotted as a function of the $\text{HOC}(\text{H}_2)$ torsion angle (τ). The blue open circles are for the complex with argon present, and the red solid ones are for the complex without argon. The large second derivative of this curve when the argon atom is present is responsible for the intensity of the overtone in the out-of-plane bend. See Supporting Information for the dependence along the b - and c -axes.

intensities of the overtone transitions in these systems are proportional to the squares of the second derivatives of these curves. Because the bend dependence of the a -component of the dipole moment is only seen when the argon atom is present, this overtone is not likely to have strong IR intensity in the bare protonated formaldehyde. The occurrence of this overtone is therefore a result of the vibrational dynamics induced by argon.

The second unexpected feature in our spectrum at 3340 cm^{-1} lies 158 cm^{-1} to the blue of the shared proton O–H stretch. This interval is comparable to the harmonic frequency of the Ar–H stretch. Analogous bands have been seen in the spectra of halide–water systems⁶¹ and protonated CO_2 .⁶² To analyze the origins of this band and, in particular, the source of its intensity, we develop an adiabatic model based on one developed by Myshakin et al.⁶³ (see Supporting Information). Using the harmonic frequencies of the O–H and Ar–H stretches along with the cubic force constant that is quadratic in the O–H stretch displacement and linear in the displacement of the Ar–H stretch, we predict an intensity of the combination band that is roughly 4% that of the OH stretch fundamental. The physical origins of the intensity comes from the fact that when the vibrational Hamiltonian is averaged over the probability amplitude for the ground and first excited states in the O–H stretch, the minimum in the resulting effective potential shifts to slightly larger values of the Ar–H distance.

We have therefore assigned all the bands measured in the photodissociation spectrum of the mass 31 cation. The most

prominent features are the fundamentals of protonated formaldehyde; additional bands are assigned to an overtone of its out-of-plane torsional mode and a combination of its O–H stretch with an argon stretch. Protonated formaldehyde has long been recognized as the most stable form of this ion, and it is therefore no surprise that it would be present. Except for the strong O–H stretch, however, none of its vibrations have been reported previously. The O–H stretch here is strongly shifted because argon attaches on the proton, but the other five fundamentals are expected to have frequencies quite close (within $5\text{--}10\text{ cm}^{-1}$) to their free-ion values. The torsional overtone (2058 cm^{-1}) and O–H/H–Ar combination (3340 cm^{-1}) band arise from the unusual vibrational dynamics resulting from attachment of argon to a cation. Our data here also provide the first spectroscopic evidence for the metastable (triplet) methoxy cation. Methoxy is present at 2–10% of the amount of protonated formaldehyde, depending on the conditions. Its survival is strongly dependent on the efficient collisional cooling in our discharge/supersonic expansion source that makes it possible to stabilize this ion behind the barriers for curve crossing to protonated formaldehyde or dissociation to $\text{HCO}^+ + \text{H}_2$. It is therefore understandable that it has been difficult to isolate this structure in the past. Like the O–H stretch of protonated formaldehyde, the C–H stretches of methoxy are perturbed significantly by the attachment of argon.

These data show that IR spectroscopy with a supersonic expansion source is useful to capture metastable ion structures resulting from complex reaction pathways and to reveal their spectral signatures. The rapid excitation followed by highly efficient collisional cooling provides a unique opportunity to sample structural configurations that are otherwise inaccessible. We have reported this behavior previously for C_3H_3^+ and C_3H_5^+ cations, both of which had coexisting isomeric structures (cyclopropenyl vs propargyl; allyl vs 2-propenyl). However, the present case is the most extreme example of this behavior yet, with triplet methoxy lying 96 kcal/mol higher in energy than protonated formaldehyde.

CONCLUSIONS

The $m/z = 31$ cation, i.e., $[\text{C}_2\text{H}_3\text{O}]^+$, has been investigated with mass-selected ion infrared photodissociation spectroscopy using the method of tagging with argon. The infrared spectrum contains sharp resonances throughout the range $1300\text{--}3500\text{ cm}^{-1}$. Spectral analysis confirms the presence of both the protonated formaldehyde and methoxy structures; there is no clear evidence for the oxonio-methylene structure suggested previously by theory. Six fundamentals are detected for protonated formaldehyde; five of these are new. The O–H stretch detected with argon tagging is strongly red-shifted compared to this vibration in the isolated cation that was reported previously. The other vibrations are believed to be less perturbed by argon and to have frequencies close to their isolated ion values. Unusual vibrational dynamics arising from the attachment of argon induces activity in the overtone of the torsion and in an argon combination with the O–H stretch. The methoxy detected is the triplet species, which is metastable with respect to protonated formaldehyde. It lies far higher in energy (computed to be $+96.0\text{ kcal/mol}$) but can be stabilized behind a significant barrier. Rapid collisional cooling in the present experiment allows this species to be captured and studied. Ion production in our pulsed discharge/supersonic expansion source provides a convenient method with which to

produce metastable ion structures and to document the IR spectra of these transient species.

■ ASSOCIATED CONTENT

■ Supporting Information

Full citation for ref 53, the computational details for the different isomeric ions considered here, mass spectra of the ions produced, absolute and relative energies, optimized geometries and normal mode frequencies, IR-PD spectra of the mass 31 cation, variation in the component of the dipole moment along the *b*- and *c*-axes, rotational temperature simulations, and analysis of the combination band at 3340 cm⁻¹. This material is available free of charge via the Internet at <http://pubs.acs.org>.

■ AUTHOR INFORMATION

Corresponding Author

*E-mail: maduncan@uga.edu.

Notes

The authors declare no competing financial interest.

■ ACKNOWLEDGMENTS

We gratefully acknowledge support for this work by the National Science Foundation through grants no. CHE-0956025 (MAD) and CHE-0848242 (ABM).

■ REFERENCES

- (1) Baer, T.; Ng, C.; Powis, I. *The Structure, Energetics and Dynamics of Organic Ions*; John Wiley & Sons: West Sussex England, 1996.
- (2) Holmes, J. L.; Aubrey, C.; Mayer, P. M. *Assigning Structures to Ions in Mass Spectrometry*; CRC Press: Boca Raton, FL, 2007.
- (3) Bowers, M. T., Ed. *Gas Phase Ion Chemistry*; Academic Press: New York, 1979; Vols. 1–3.
- (4) Carrington, A.; Thrush, B. A., Eds. *The Spectroscopy of Molecular Ions*; The Royal Society: London, 1988.
- (5) Duncan, M. A. *Int. J. Mass Spectrom.* **2000**, *200*, 545–569.
- (6) Hartquist, T. W.; Williams, D. A. *The Molecular Astrophysics of Stars and Galaxies*; Clarendon Press: Oxford, U.K., 1998.
- (7) Tielens, A. G. G. M. *The Physics and Chemistry of the Interstellar Medium*; Cambridge University Press: Cambridge, U.K., 2005.
- (8) Petrie, S.; Bohme, D. K. *Mass Spectrom. Rev.* **2007**, *26*, 258–280.
- (9) Snow, T. P.; Bierbaum, V. M. *Annu. Rev. Anal. Chem.* **2008**, *1*, 229–259.
- (10) (a) Okumura, M.; Yeh, L. I.; Myers, J. D.; Lee, Y. T. *J. Chem. Phys.* **1986**, *85*, 2328–2329. (b) Okumura, M.; Yeh, L. I.; Myers, J. D.; Lee, Y. T. *J. Phys. Chem.* **1990**, *94*, 3416–3427.
- (11) Ebata, T.; Fujii, A.; Mikami, N. *Int. Rev. Phys. Chem.* **1998**, *17*, 331–361.
- (12) Bieske, E. J.; Dopfer, O. *Chem. Rev.* **2000**, *100*, 3963–3998.
- (13) Robertson, W. H.; Johnson, M. A. *Annu. Rev. Phys. Chem.* **2003**, *54*, 173–213.
- (14) Duncan, M. A. *Int. Rev. Phys. Chem.* **2003**, *22*, 407–435.
- (15) Baer, T.; Dunbar, R. C. *J. Am. Soc. Mass Spectrom.* **2010**, *21*, 681–693.
- (16) Doublerly, G. E.; Ricks, A. M.; Ticknor, B. W.; McKee, W. C.; Schleyer, P. v. R.; Duncan, M. A. *J. Phys. Chem. A* **2008**, *112*, 1897–1906.
- (17) Ricks, A. M.; Doublerly, G. E.; Schleyer, P. v. R.; Duncan, M. A. *J. Chem. Phys.* **2010**, *132*, 051101/1–4.
- (18) Doublerly, G. E.; Ricks, A. M.; Schleyer, P. v. R.; Duncan, M. A. *J. Chem. Phys.* **2008**, *128*, 021102/1–4.
- (19) Doublerly, G. E.; Ricks, A. M.; Ticknor, B. W.; Schleyer, P. v. R.; Duncan, M. A. *J. Phys. Chem. A* **2008**, *112*, 4869–4874.
- (20) Ricks, A. M.; Doublerly, G. E.; Duncan, M. A. *Astrophys. J.* **2009**, *702*, 301–306.
- (21) NIST Mass Spec Data Center, S. E. Stein, director. Mass Spectra. In *NIST Chemistry WebBook*; Linstrom, P. J., Mallard, W. G., Eds.; NIST Standard Reference Database Number 69; National Institute of Standards and Technology: Gaithersburg, MD, 20899, <http://webbook.nist.gov> (retrieved May 14, 2012).
- (22) Munson, M. S. B.; Franklin, J. L. *J. Phys. Chem.* **1964**, *68*, 3191–3194.
- (23) Haney, M. A.; Patel, J. C.; Hayes, E. F. *J. Chem. Phys.* **1970**, *53*, 4105–4106.
- (24) Bowen, R. D.; Williams, D. H. *J. Chem. Soc., Chem. Commun.* **1977**, 378–380.
- (25) Schleyer, P. v. R.; Jemmis, E. D. *J. Chem. Soc., Chem. Commun.* **1978**, 190–191.
- (26) Dill, J. D.; Fischer, C. L.; McLafferty, F. W. *J. Am. Chem. Soc.* **1979**, *101*, 6531–6534.
- (27) Bursey, M. M.; Hass, J. R.; Harvan, D. J.; Parker, C. E. *J. Am. Chem. Soc.* **1979**, *101*, 5485–5489.
- (28) Nobes, R. H.; Radom, L.; Rodwell, W. R. *Chem. Phys. Lett.* **1980**, *74*, 269–272.
- (29) Hoffmann, M. R.; Schaefer, H. F. *Astrophys. J.* **1981**, *249*, 563–565.
- (30) Bouma, W. J.; Nobes, R. H.; Radom, L. *Org. Mass Spectrom.* **1982**, *17*, 315–317.
- (31) Gilman, J. P.; Hsieh, T.; Meissels, G. G. *J. Chem. Phys.* **1983**, *78*, 3767–3773.
- (32) Burgers, P. C.; Holmes, J. L. *Org. Mass Spectrom.* **1984**, *19*, 452–456.
- (33) Holmes, J. L.; Terlouw, J. K. *Org. Mass Spectrom.* **1986**, *21*, 776–778.
- (34) Zappey, H. W.; Ingemann, S.; Nibbering, N. M. M. *J. Am. Soc. Mass Spectrom.* **1992**, *3*, 515–517.
- (35) Uggerud, E.; Helgaker, T. *J. Am. Chem. Soc.* **1992**, *114*, 4265–4268.
- (36) Yarkony, D. R. *J. Am. Chem. Soc.* **1992**, *114*, 5406–5411.
- (37) Kuo, S.-C.; Zhang, Z.; Klemm, R. B.; Liebman, J. F.; Stief, L. J.; Nesbitt, F. L. *J. Phys. Chem.* **1994**, *98*, 4026–4033.
- (38) Lee, T. G.; Park, S. C.; Kim, M. S. *J. Chem. Phys.* **1996**, *104*, 4517–4529.
- (39) Suárez, D.; Sordo, T. L. *J. Phys. Chem. A* **1997**, *101*, 1561–1566.
- (40) Aschi, M.; Harvey, J. N.; Schalley, C. A.; Schröder, D.; Schwarz, H. *Chem. Commun.* **1998**, 531–533.
- (41) Harvey, J. N.; Aschi, M. *Phys. Chem. Chem. Phys.* **1999**, *1*, 5555–5563.
- (42) Zhu, X. J.; Ge, M. F.; Wang, J.; Sun, Z.; Wang, D. X. *Angew. Chem., Int. Ed.* **2000**, *39*, 1940–1943.
- (43) Amano, T.; Warner, H. E. *Astrophys. J.* **1989**, *342*, L99–L101.
- (44) Dore, L.; Cazzoli, G.; Civis, S.; Scappini, F. *Chem. Phys. Lett.* **1995**, *244*, 145–148.
- (45) Ohishi, M.; Ishikawa, S.; Amano, T.; Oka, H.; Irvine, W. M.; Dickens, J. E.; Ziurys, L. M.; Apponi, A. J. *Astrophys. J.* **1996**, *471*, L61–L64.
- (46) Del Bene, J. E.; Gwaltney, S. R.; Bartlett, R. J. *J. Phys. Chem. A* **1998**, *102*, 5124–5127.
- (47) Blowers, P.; Masel, R. I. *J. Phys. Chem. A* **2000**, *104*, 34–44.
- (48) Castro, M. E.; Nino, A.; Munoz-Caro, C. *Theo. Chem. Acc.* **2008**, *119*, 343–354.
- (49) Sears, K. C.; Ferguson, J. W.; Dudley, T. J.; Houk, R. S.; Gordon, M. S. *J. Phys. Chem. A* **2008**, *112*, 2610–2617.
- (50) Cornett, D. S.; Peschke, M.; LaiHing, K.; Cheng, P. Y.; Willey, K. F.; Duncan, M. A. *Rev. Sci. Instrum.* **1992**, *63*, 2177–2186.
- (51) Bosenberg, W. R.; Guyer, D. R. *J. Opt. Soc. Am. B* **1993**, *10*, 1716–1722.
- (52) Gerhards, M.; Unterberg, C.; Gerlach, A. *Phys. Chem. Chem. Phys.* **2002**, *4*, 5563–5565.
- (53) Frisch, M. J.; et al. *Gaussian 03*, Revision B.02; Gaussian, Inc.: Pittsburgh, PA, 2003.
- (54) Merrick, J. P.; Moran, D.; Radom, L. *J. Phys. Chem. A* **2007**, *111*, 11683–11700.
- (55) Shimanouchi, T. *Molecular Vibrational Frequencies*. *NIST Chemistry WebBook*; Linstrom, P. J., Mallard, W. G., Eds.; NIST Standard Reference Database Number 69; National Institute of

Standards and Technology: Gaithersburg, MD, 20899 (<http://webbook.nist.gov>).

(56) Dulcey, C. S.; Hudgens, J. W. *J. Chem. Phys.* **1986**, *84*, 5262–5270.

(57) Johnson, R. D.; Hudgens, J. W. *J. Phys. Chem.* **1996**, *100*, 19874–19890.

(58) Dyke, J. M.; Ellis, A. R.; Jonathan, N.; Keddar, N.; Morris, A. *Chem. Phys. Lett.* **1984**, *111*, 207–210.

(59) Botschwina, P.; Oswald, R. *J. Chem. Phys.* **2011**, *134*, 044305/1–6.

(60) Roscioli, J. R.; Diken, E. G.; Johnson, M. A.; Horvath, S.; McCoy, A. B. *J. Phys. Chem. A* **2006**, *110*, 4943–4952.

(61) Horvath, S.; McCoy, A. B.; Eliot, B. M.; Weddle, G. H.; Roscioli, J. R.; Johnson, M. A. *J. Phys. Chem. A* **2010**, *115*, 1556–1568.

(62) Douberly, G. E.; Ricks, A. M.; Ticknor, B. W.; Duncan, M. A. *J. Phys. Chem. A* **2008**, *112*, 950–959.

(63) Myshakin, E. M.; Jordan, K. D.; Sibert, E. L.; Johnson, M. A. *J. Chem. Phys.* **2003**, *119*, 10138.